

Faddeev Calculation of Hypertriton Including with YNN Three-Body Force

H. Kamada (Kyushu Institute of Technology + RCNP, Japan),
M. Kohno (Osaka University RCNP, Japan),
K. Miyagawa (Osaka University RCNP, Japan)



Chiral Dynamics 2024

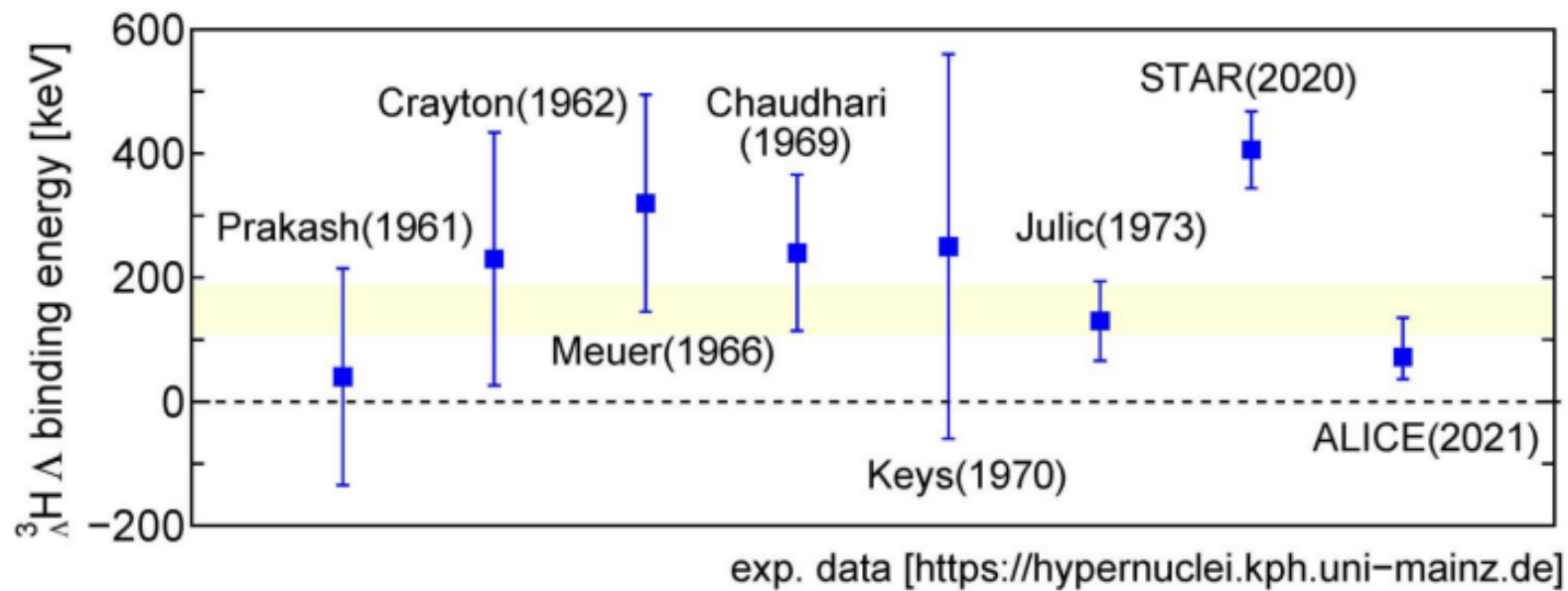
2024 Aug. 26 Rhur Universitaet Bochum, Germany

hypertriton (${}^3_{\Lambda}\text{H}$)

The first bound hypernucleus

➤ Average bond energy

$$162 \pm 44 \text{ keV}$$



hypertriton (${}^3_{\Lambda}\text{H}$)

➤ Lifetime

Measurement of the Lifetime and Λ Separation Energy of ${}^3_{\Lambda}\text{H}$

S. Acharya *et al.*^{*}
(ALICE Collaboration)

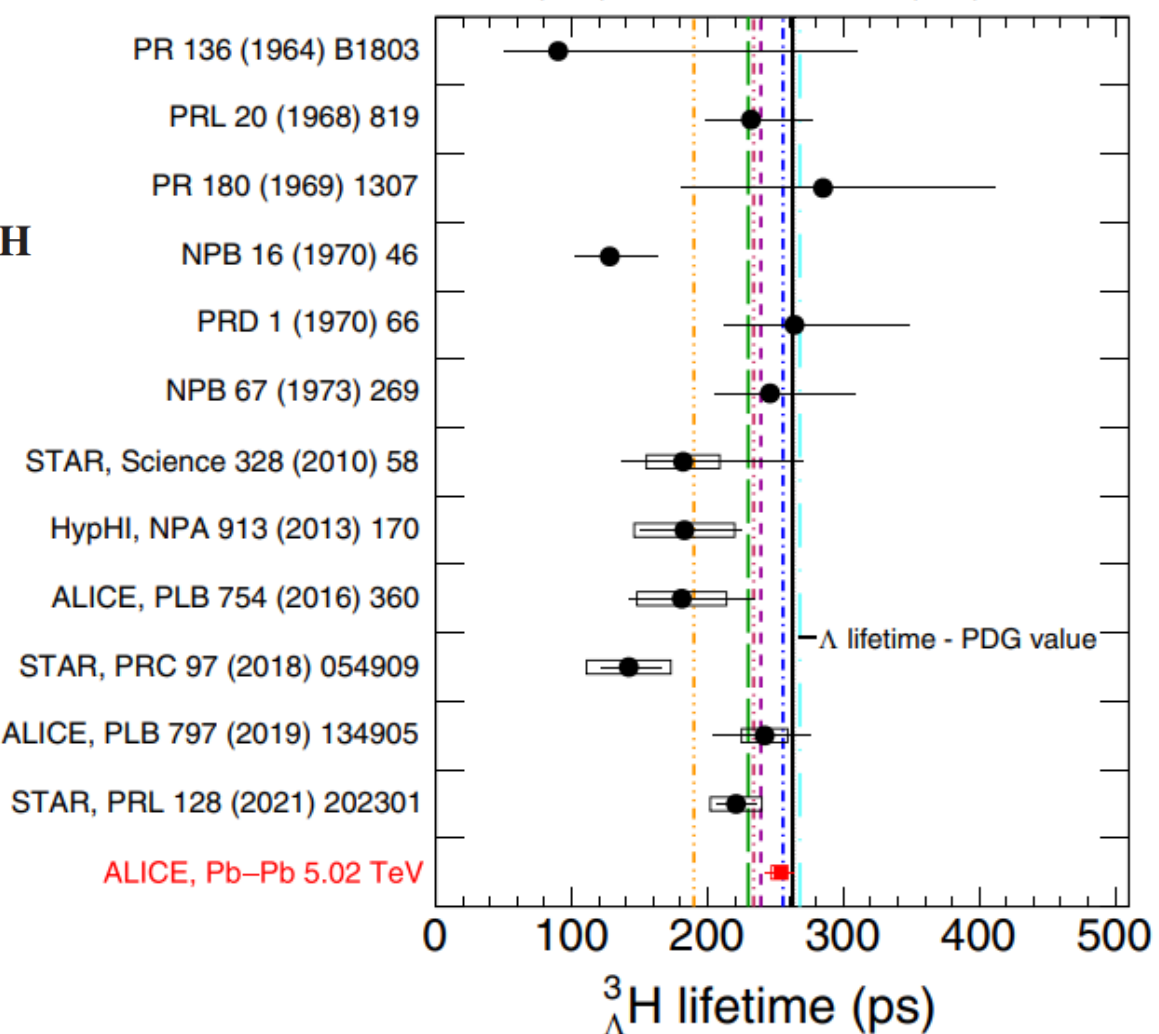
PHYSICAL REVIEW LETTERS 131, 102302 (2023)

π -mesonic decay of the hypertriton

H. Kamada, J. Golak, K. Miyagawa, H. Witała, and W. Glöckle
Phys. Rev. C **57**, 1595 – Published 1 April 1998

Theoretical predictions

- Nuo. Cim. 46 (1966) 786
- PRC 57 (1998) 1595
- PLB 811 (2020) 135916 - A
- J.Phys. G18 (1992) 339-357
- PRC 102 (2020) 064002
- PLB 811 (2020) 135916 - B



Faddeev Equations for the Hypertriton bound state (no 3-body force)

[K. Miyagawa, H. Kamada, W. Glöckle, and V. Stoks, Phys. Rev. C 51, 2905 (1995)]

- Λ NN Schrödinger Eq. ; 2body force V_{ij} , Kinetic term H_0

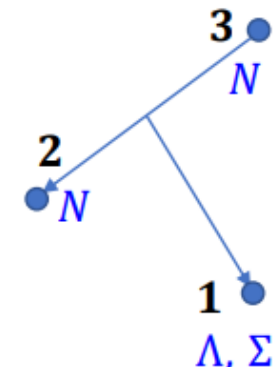
$$(H_0 + V_{12} + V_{23} + V_{31})\Psi = E\Psi \xrightarrow{\text{L-S eq.}} \Psi = \frac{1}{E - H_0}(V_{12} + V_{23} + V_{31})\Psi \equiv \psi_{12} + \psi_{23} + \psi_{31}$$

- $G_0 \equiv \frac{1}{E - H_0}$, t-matrix $t_{ij} = V_{ij} + V_{ij}G_0t_{ij}$ $P_{23}\psi_{12} = -\psi_{31}$
- $\psi_{12} = G_0t_{12}(\psi_{23} - P_{23}\psi_{12})$ and $\psi_{23} = G_0t_{23}(1 - P_{23})\psi_{12}$

- ψ_{ij} consists of Λ channel and Σ channel

$$\begin{pmatrix} \psi_{\Lambda}^{(12)} \\ \psi_{\Sigma}^{(12)} \end{pmatrix} = \begin{pmatrix} \{E - H_0(NN\Lambda)\}^{-1} & 0 \\ 0 & \{E - H_0(NN\Sigma)\}^{-1} \end{pmatrix} \begin{pmatrix} t_{12}^{\Lambda} & 0 \\ 0 & t_{12}^{\Sigma} \end{pmatrix} \left[\begin{pmatrix} \psi_{\Lambda}^{(23)} \\ \psi_{\Sigma}^{(23)} \end{pmatrix} - \begin{pmatrix} P_{23}\psi_{\Lambda}^{(12)} \\ P_{23}\psi_{\Sigma}^{(12)} \end{pmatrix} \right]$$

$$\begin{pmatrix} \psi_{\Lambda}^{(23)} \\ \psi_{\Sigma}^{(23)} \end{pmatrix} = \begin{pmatrix} \{E - H_0(NN\Lambda)\}^{-1} & 0 \\ 0 & \{E - H_0(NN\Sigma)\}^{-1} \end{pmatrix} \begin{pmatrix} t_{23}^{\Lambda} & 0 \\ 0 & t_{23}^{\Sigma} \end{pmatrix} \begin{pmatrix} (1 - P_{23})\psi_{\Lambda}^{(12)} \\ (1 - P_{23})\psi_{\Sigma}^{(12)} \end{pmatrix}$$



Faddeev Equations including with 3body force

- A NN Schrödinger Eq. ; 2body force V_{ij} , Kinetic term H_0 , 3-body force W

$$(H_0 + V_{12} + V_{23} + V_{31} + W)\Psi = E\Psi$$
- Green func. $G_0 \equiv \frac{1}{E - H_0}$ Lippmann-Schwinger eq. $\Psi = G_0(V_{12} + V_{23} + V_{31} + W)\Psi$
- Faddeev Components : $\Psi = \psi_{12} + \psi_{23} + \psi_{31}$ $i = 1$ = Hyperon
 $\psi_{12} \equiv G_0 V_{12} \Psi, \quad \psi_{23} \equiv G_0 (V_{23} + W) \Psi, \quad \psi_{31} \equiv G_0 V_{31} \Psi$
- t-matrix ; $t_{ij} = V_{ij} + V_{ij} G_0 t_{ij}$ Möller Oper.; $\Omega_{ij} \equiv (1 - G_0 V_{ij})^{-1} = (1 + G_0 t_{ij})$

$$\begin{cases} \psi_{12} = G_0 t_{12} (\psi_{23} + \psi_{31}) \\ \psi_{23} = G_0 t_{23} (\psi_{12} + \psi_{31}) + (G_0 + G_0 t_{23} G_0) W (\psi_{12} + \psi_{23} + \psi_{31}) \\ \psi_{31} = G_0 t_{31} (\psi_{12} + \psi_{23}) \end{cases} : \psi_{ij} = \begin{pmatrix} \psi_{\Lambda}^{(ij)} \\ \psi_{\Sigma}^{(ij)} \end{pmatrix}$$

[$\psi_{31} = -P_{12}\psi_{23}$]

INPUT

- 2body force (NN) : Chiral forces N⁴LO+ [Cut off scale; 400,450,500,550 MeV]
- 2body force (YN) : Chiral forces (Juelich) NLO13,NLO19 [Cut off 550, 600, 650 MeV]
- 3body force (YNN) : 2pi exchange type

J. Haidenbauer, S. Petschauer, N. Kaiser, U.-G. Meißner, A. Nogga, and W. Weise, Hyperon-nucleon interaction at next-to-leading order in chiral effective field theory, [Nucl. Phys. A 915, 24 \(2013\)](#).

J. Haidenbauer, U.-G. Meißner, and A. Nogga, Hyperon-nucleon interaction within chiral effective field theory revisited, [Eur. Phys. J. A 56, 91 \(2020\)](#).

P. M. M. Maessen, Th. A. Rijken, and J. J. de Swart,
Soft-core baryon-baryon one-boson-exchange models.
II. Hyperon-nucleon potential, [Phys. Rev. C 40, 2226 \(1989\)](#).

NN Potential
N⁴LO+

NLO13(550)

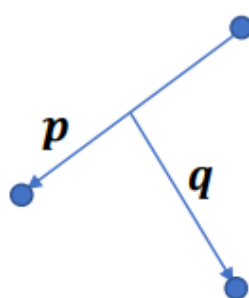
NLO19(550),NLO19(600),
NLO19(650)

NSC89

Λ N Potential

P. Reinert, and H. Krebs, and E. Epelbaum, Semilocal momentum-space regularized chiral two-nucleon potentials up to fifth order, [Eur. Phys. J. A 54, 86 \(2018\)](#).

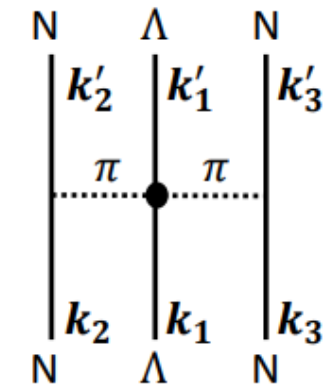
3-body force (YNN): 2π exchange type



$$V_{TPE}^{\Lambda NN} = \frac{g_A^2}{3f_0^4} (\boldsymbol{\tau}_2 \cdot \boldsymbol{\tau}_3) \frac{(\boldsymbol{\sigma}_3 \cdot \mathbf{q}_{3d})(\boldsymbol{\sigma}_2 \cdot \mathbf{q}_{2d})}{(\mathbf{q}_{3d}^2 + m_\pi^2)(\mathbf{q}_{2d}^2 + m_\pi^2)} \{-Am_\pi^2 + B\mathbf{q}_{3d} \cdot \mathbf{q}_{2d}\}$$

$$\mathbf{q}_{2d} = \mathbf{k}'_2 - \mathbf{k}_2 = \mathbf{p}'_1 - \mathbf{p}_1 - \frac{1}{2}(\mathbf{q}'_1 - \mathbf{q}_1) \equiv \mathbf{p} - \frac{1}{2}\mathbf{q}$$

$$\mathbf{q}_{3d} = \mathbf{k}'_3 - \mathbf{k}_3 = -(\mathbf{p}'_1 - \mathbf{p}_1) - \frac{1}{2}(\mathbf{q}'_1 - \mathbf{q}_1) \equiv -\mathbf{p} - \frac{1}{2}\mathbf{q}$$



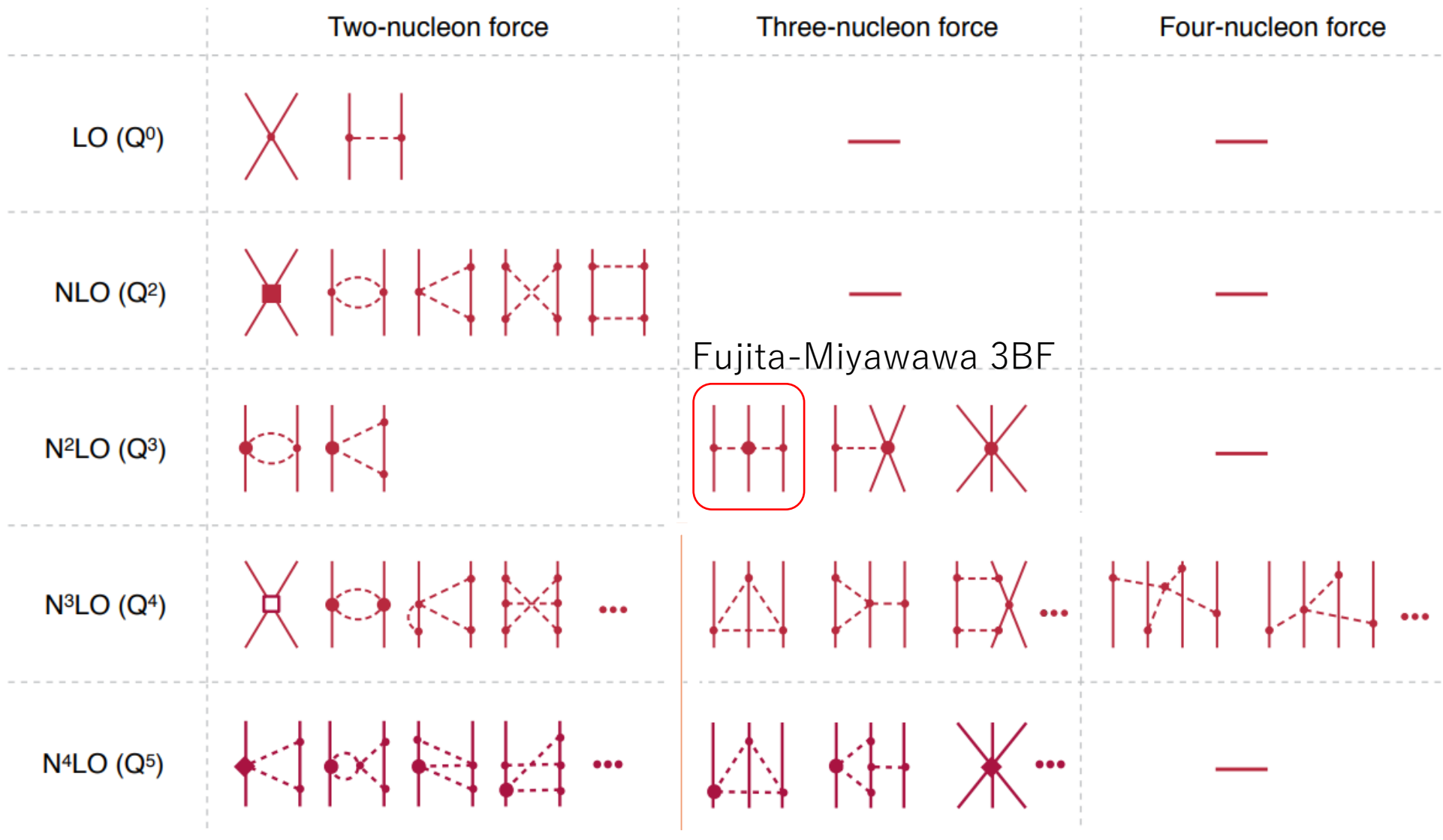
- The two parameters A and B should be determined by the NNLO LEC, but here they were estimated by the Isobar-saturation model.

[Petschauer *et al.*, Phys. Rev. C 93, 014001 (2016)] $A = 0, B = -3.0 \text{ GeV}^{-1}$

NNLO fit [Haidenbauer *et al.*, Eur. Phys. J. A (2024) 6:3] $A=1.485, B=-3.01\text{GeV}^{-1}$



Calculation Results



The 3-body force is decomposed into the partial waves.

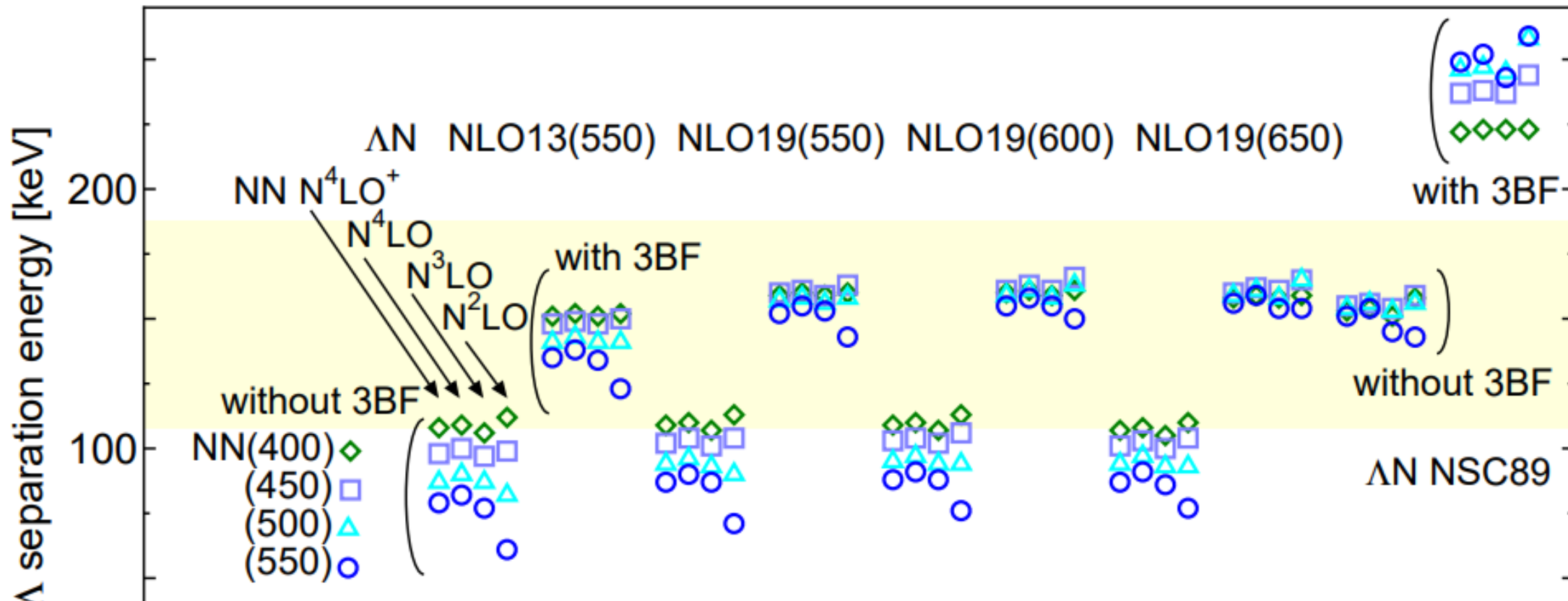
$$\begin{aligned}
& \langle \{ [Y_{\ell'_d}(\hat{\mathbf{p}}'_1) \times \chi_d^1]^1 \times [Y_{\ell'_\Lambda}(\hat{\mathbf{q}}'_1) \times \chi_\Lambda^{1/2}]^{j_\Lambda} \}_{M_t}^{J_t} | V_{\text{TPE}}^{(K, \ell_a, \ell_b)}(p, q) \{ [Y_{\ell_a}(\hat{\mathbf{p}}) \times Y_{\ell_b}(\hat{\mathbf{q}})]^K \times [\sigma_2 \times \sigma_3]^K \}_0^0 \\
& \quad \times | \{ [Y_{\ell_d}(\hat{\mathbf{p}}_1) \times \chi_d^1]^1 \times [Y_{\ell_\Lambda}(\hat{\mathbf{q}}_1) \times \chi_\Lambda^{1/2}]^{j_\Lambda} \}_{M_t}^{J_t} \} \\
& = \sum_{L'L} \sum_{S'S} 3 \hat{j}_\Lambda \sqrt{\hat{L}' \hat{S}' \hat{L} \hat{S}} \left\{ \begin{array}{ccc} \ell'_d & \ell_{\Lambda'} & L' \\ 1 & 1/2 & S' \\ 1 & j_{\Lambda'} & J_t \end{array} \right\} \left\{ \begin{array}{ccc} \ell_d & \ell_\Lambda & L \\ 1 & 1/2 & S \\ 1 & j_\Lambda & J_t \end{array} \right\} \langle \{ [Y_{\ell'_d}(\hat{\mathbf{p}}'_1) \times Y_{\ell'_\Lambda}(\hat{\mathbf{q}}'_1)]^{L'} \times [\chi_d^1 \times \chi_\Lambda^{1/2}]^{S'} \}_{M_t}^{J_t} | \\
& \quad \times V_{\text{TPE}}^{(K, \ell_a, \ell_b)}(p, q) \{ [Y_{\ell_a}(\hat{\mathbf{p}}) \times Y_{\ell_b}(\hat{\mathbf{q}})]^K \times [\sigma_2 \times \sigma_3]^K \}_0^0 | \{ [Y_{\ell_d}(\hat{\mathbf{p}}_1) \times Y_{\ell_\Lambda}(\hat{\mathbf{q}}_1)]^L \times [\chi_d^1 \times \chi_\Lambda^{1/2}]^S \}_{M_t}^{J_t} \} \\
& = \sum_{L'L} \sum_{S'S} 3 \hat{j}_\Lambda \sqrt{\hat{L}' \hat{S}' \hat{L} \hat{S}} \left\{ \begin{array}{ccc} \ell'_d & \ell_{\Lambda'} & L' \\ 1 & 1/2 & S' \\ 1 & j_{\Lambda'} & J_t \end{array} \right\} \left\{ \begin{array}{ccc} \ell_d & \ell_\Lambda & L \\ 1 & 1/2 & S \\ 1 & j_\Lambda & J_t \end{array} \right\} \sqrt{\hat{j}_t \hat{L}' \hat{S}'} \left\{ \begin{array}{ccc} J_t & J_t & 0 \\ L' & L & K \\ S' & S & K \end{array} \right\} \langle [Y_{\ell'_d}(\hat{\mathbf{p}}'_1) \times Y_{\ell'_\Lambda}(\hat{\mathbf{q}}'_1)]^{L'} | V_{\text{TPE}}^{(K, \ell_a, \ell_b)}(p, q) \\
& \quad \times [Y_{\ell_a}(\hat{\mathbf{p}}) \times Y_{\ell_b}(\hat{\mathbf{q}})]^K | [Y_{\ell_d}(\hat{\mathbf{p}}_1) \times Y_{\ell_\Lambda}(\hat{\mathbf{q}}_1)]^L \rangle_{pwe} 18 \sqrt{\hat{S} \hat{K}} (-1)^{K+3/2+S} \left\{ \begin{array}{ccc} S' & S & K \\ 1 & 1 & 1/2 \end{array} \right\} \left\{ \begin{array}{ccc} 1 & 1 & K \\ 1/2 & 1/2 & 1 \\ 1/2 & 1/2 & 1 \end{array} \right\},
\end{aligned}$$

TABLE II. Hypertriton separation energies without 3BFs. Entries are in keV. The numbers in parentheses for NN and YN chiral potentials indicate the cutoff scale Λ_c in MeV.

NN potential (Λ_c)	YN potential (Λ_c)				
	NLO13 (550)	NLO19 (550)	NLO19 (600)	NLO19 (650)	NSC89
CDBonn [23]	82	90	90	88	153
Nijmegen 93 [32]	58	69	70	70	141
Nijmegen I [32]	63	75	75	74	145
$N^4\text{LO}+$ (550)	79	87	88	87	151
$N^4\text{LO}+$ (500)	87	94	95	94	154
$N^4\text{LO}+$ (450)	98	102	103	101	155
$N^4\text{LO}+$ (400)	108	109	109	107	153
$N^4\text{LO}$ (550)	82	90	91	91	154
$N^4\text{LO}$ (500)	90	96	97	97	156
$N^4\text{LO}$ (450)	100	104	104	103	156
$N^4\text{LO}$ (400)	109	110	110	108	154
$N^3\text{LO}$ (550)	77	87	88	86	145
$N^3\text{LO}$ (500)	87	93	94	93	153
$N^3\text{LO}$ (450)	97	101	102	100	154
$N^3\text{LO}$ (400)	106	107	107	105	151
$N^2\text{LO}$ (550)	61	71	76	77	143
$N^2\text{LO}$ (500)	82	90	94	93	156
$N^2\text{LO}$ (450)	99	104	106	104	159
$N^2\text{LO}$ (400)	112	113	113	110	158

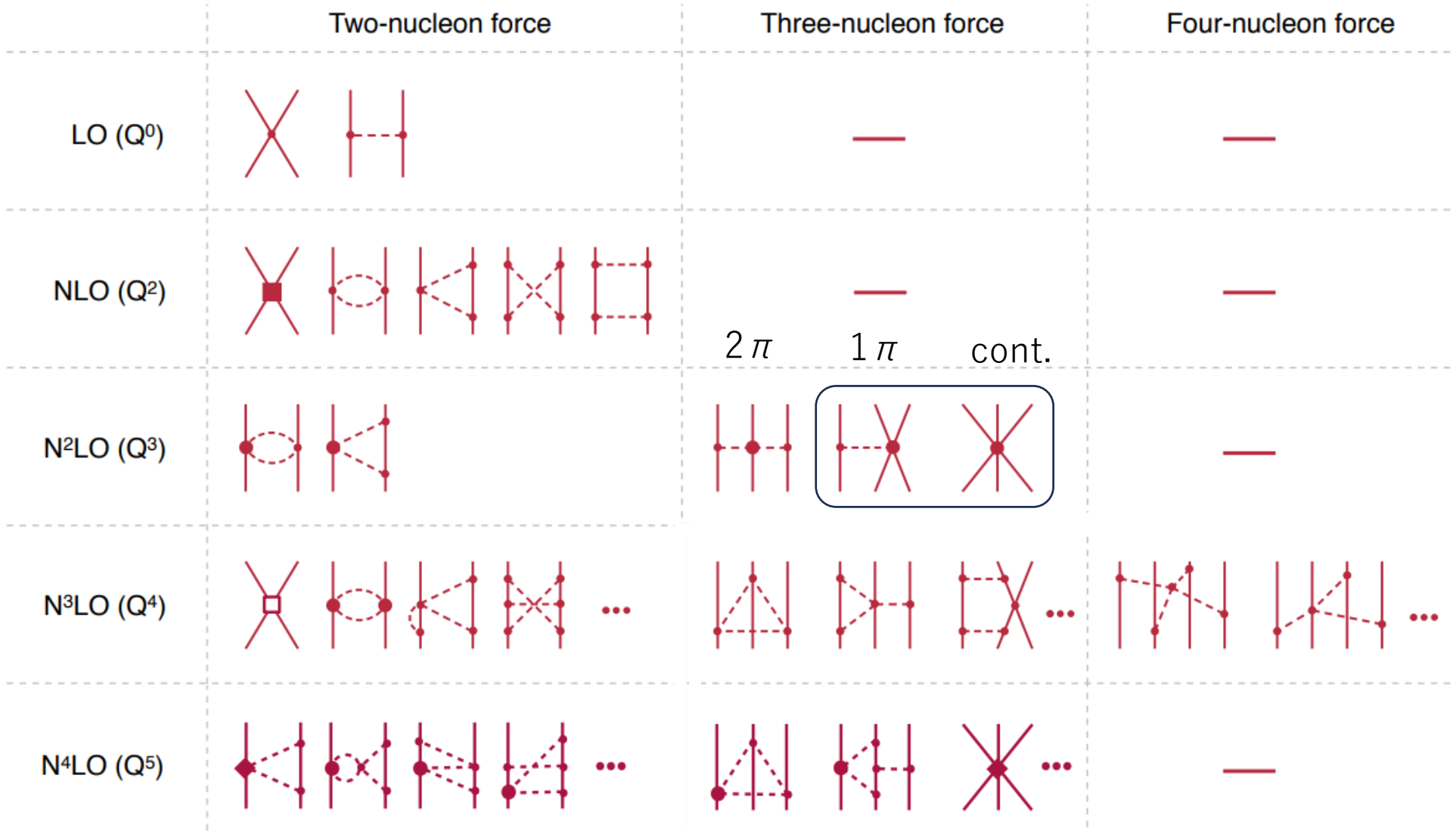
Table I: Hypertriton separation energies that include 2π -exchange ANN 3BF with $3b_0 + b_D = 0$ and $2b_2 + 3b_4 = -3.0 \text{ GeV}^{-1}$. Entries are in keV. The numbers in parentheses for NN and YN chiral potentials indicate the cutoff scale Λ_c in MeV.

NN potential (Λ_c)	YN potential (Λ_c)				
	NLO13 (550)	NLO19 (550)	NLO19 (600)	NLO19 (650)	NSC89
CDBonn [9]	135	151	151	151	244
Nijmegen 93 [10]	114	135	138	140	249
Nijmegen I [10]	120	142	144	145	252
$N^4\text{LO}+$ (550)	135	152	155	156	249
$N^4\text{LO}+$ (500)	141	157	159	159	246
$N^4\text{LO}+$ (450)	148	160	161	160	237
$N^4\text{LO}+$ (400)	151	159	160	158	222
$N^4\text{LO}$ (550)	138	155	158	159	252
$N^4\text{LO}$ (500)	143	158	161	161	247
$N^4\text{LO}$ (450)	149	161	163	162	238
$N^4\text{LO}$ (400)	152	160	161	159	223
$N^3\text{LO}$ (550)	134	153	155	154	243
$N^3\text{LO}$ (500)	141	156	158	158	245
$N^3\text{LO}$ (450)	148	159	161	161	237
$N^3\text{LO}$ (400)	151	159	159	158	223
$N^2\text{LO}$ (550)	123	143	150	154	259
$N^2\text{LO}$ (500)	141	158	163	165	258
$N^2\text{LO}$ (450)	150	163	166	165	244
$N^2\text{LO}$ (400)	152	160	161	159	223



[Kamada, Kohno, Miyagawa: PHYSICAL REVIEW C 108, 024004 (2023)]

3 N System

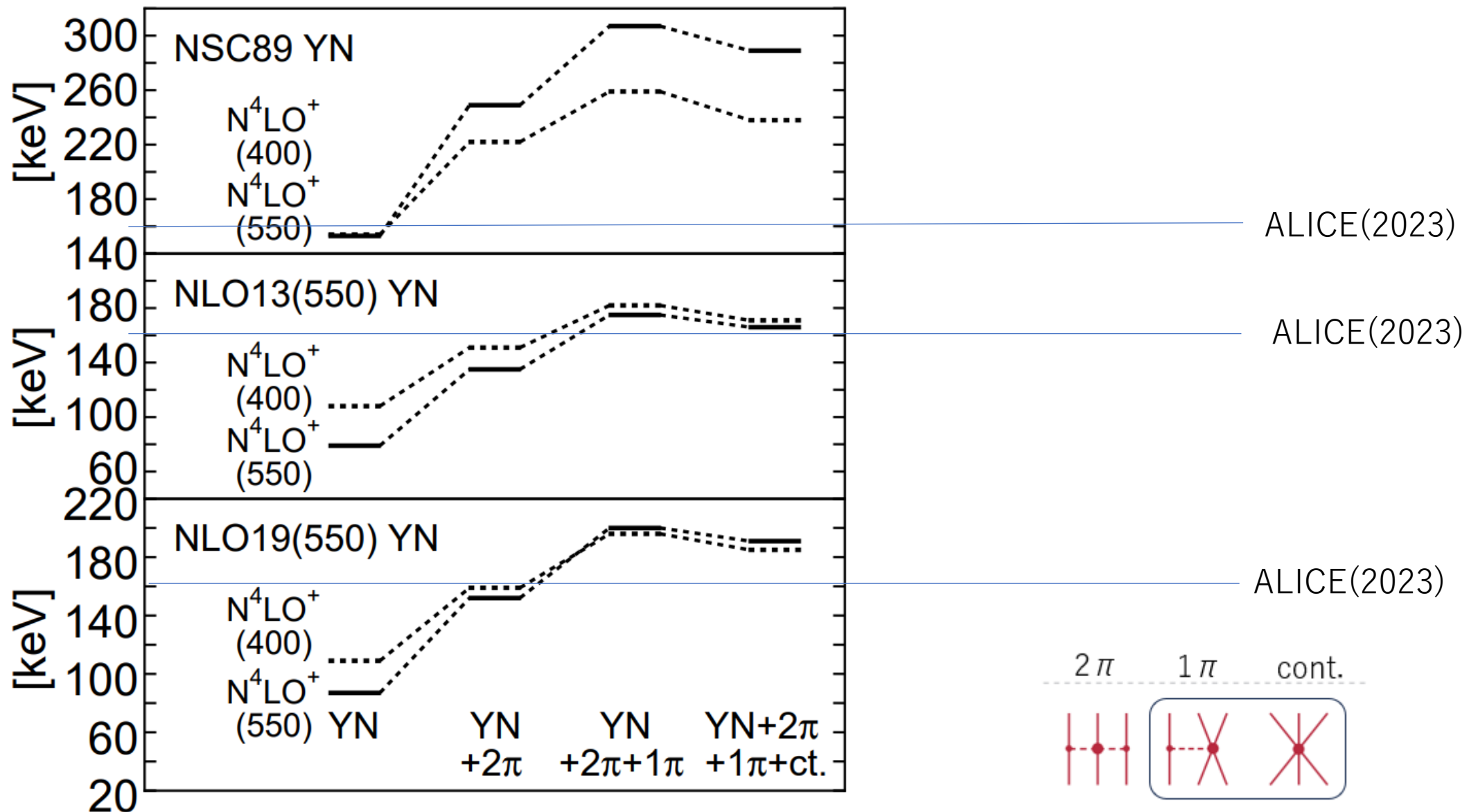


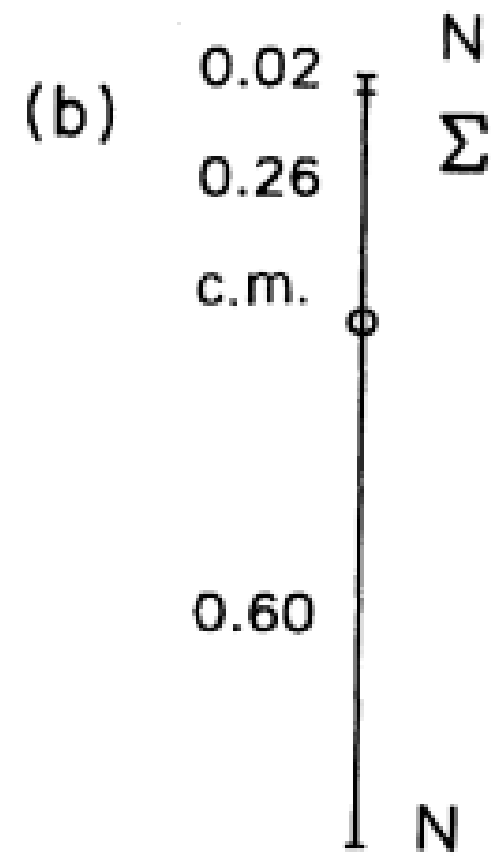
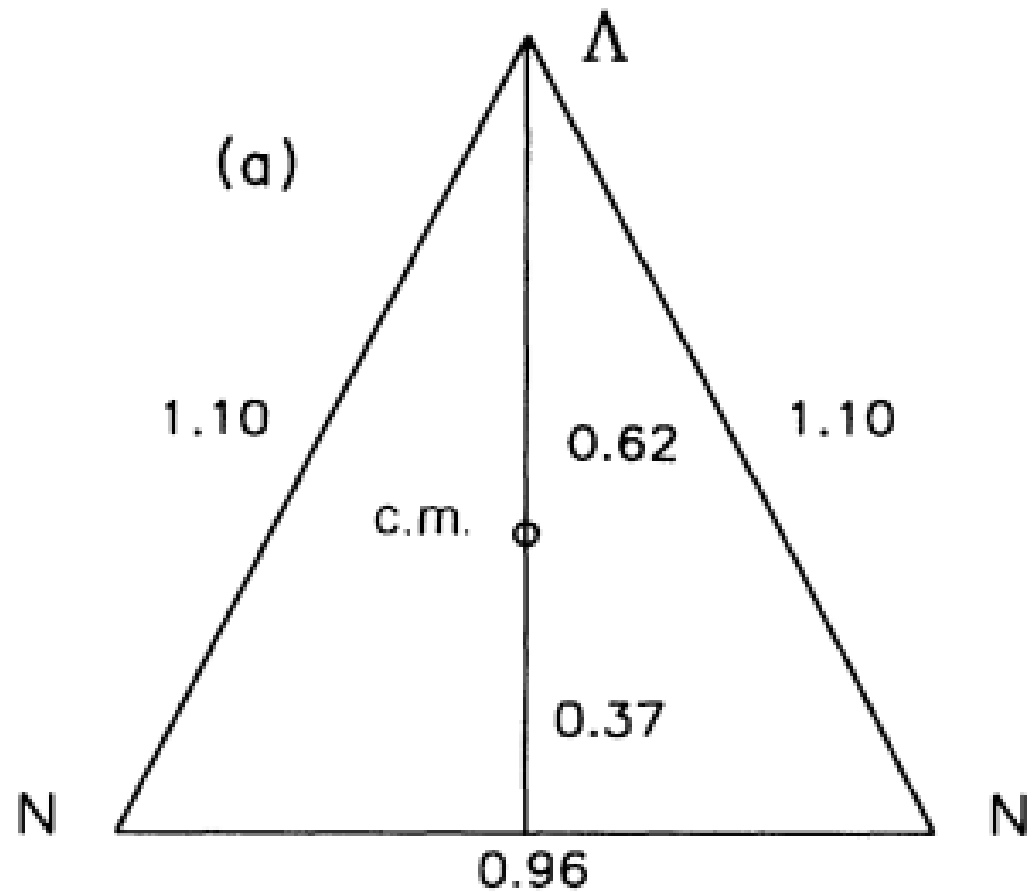
+ 2 π + 1 π

+ 2 π + 1 π + cont.

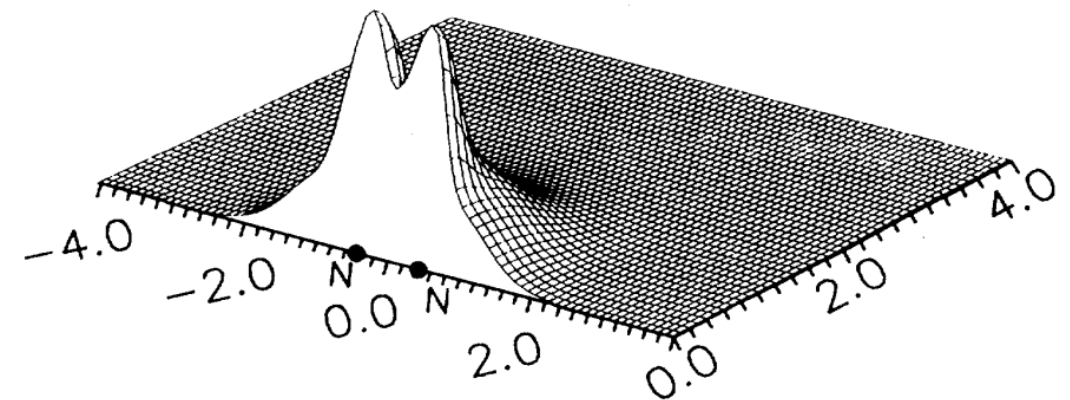
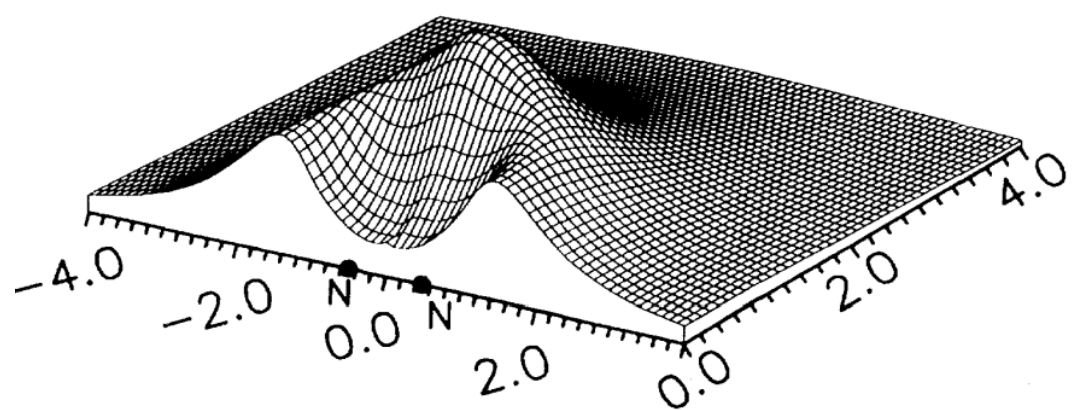
NN potential (Λ_c)	YN potential (Λ_c)				
	NLO13 (550)	NLO19 (550)	NLO19 (600)	NLO19 (650)	NSC89
CDBonn [23]	172	194	196	196	317
Nijmegen 93 [32]	114	183	187	191	313
Nijmegen I [32]	120	191	194	196	315
N^4LO+ (550)	175	200	204	205	307
N^4LO+ (500)	180	202	205	206	299
N^4LO+ (450)	183	201	204	203	283
N^4LO+ (400)	182	196	197	196	259
N^4LO (550)	178	201	206	208	309
N^4LO (500)	182	203	207	208	300
N^4LO (450)	184	202	205	205	283
N^4LO (400)	183	196	198	197	259
N^3LO (550)	175	200	204	204	300
N^3LO (500)	180	201	205	206	298
N^3LO (450)	184	202	205	205	284
N^3LO (400)	182	196	198	197	261
N^2LO (550)	167	195	205	210	330
N^2LO (500)	183	207	214	216	318
N^2LO (450)	187	206	210	210	292
N^2LO (400)	182	195	197	194	257

NN potential (Λ_c)	YN potential (Λ_c)				
	NLO13 (550)	NLO19 (550)	NLO19 (600)	NLO19 (650)	NSC89
CDBonn [23]	163	185	187	187	300
Nijmegen 93 [32]	148	176	180	183	296
Nijmegen I [32]	154	183	186	187	298
N^4LO+ (550)	166	191	195	196	289
N^4LO+ (500)	170	192	196	196	280
N^4LO+ (450)	173	191	194	193	263
N^4LO+ (400)	171	185	187	184	238
N^4LO (550)	169	192	197	206	290
N^4LO (500)	172	193	197	198	280
N^4LO (450)	174	192	195	194	263
N^4LO (400)	172	185	187	185	239
N^3LO (550)	166	191	195	195	281
N^3LO (500)	171	192	195	196	279
N^3LO (450)	173	191	194	194	264
N^3LO (400)	172	186	187	185	241
N^2LO (550)	188	188	198	203	314
N^2LO (500)	198	198	207	207	300
N^2LO (450)	195	195	200	199	271
N^2LO (400)	184	184	186	182	236





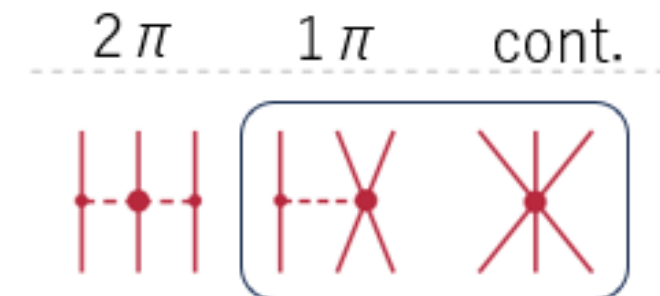
[K. Miyagawa, H. Kamada, W. Glöckle, and V. Stoks, Phys. Rev. C 51, 2905 (1995)]



[K. Miyagawa, H. Kamada, W. Glöckle, and V. Stoks, Phys. Rev. C 51, 2905 (1995)]

Probabilities of Deuteron and Σ particle in Hypertriton

	Nijm93 NSC89	N^4LO+ NLO19	N^4LO+ NLO19 2pi 3BF	N^4LO+ NLO19 2pi+1pi 3BF	N^4LO+ NLO19 2pi+1pi+cnt. 3BF
Σ prob.	0.0047	0.0019	0.0026	0.0031	0.0030
Deuteron prob.	0.880	0.891	0.887	0.883	0.884



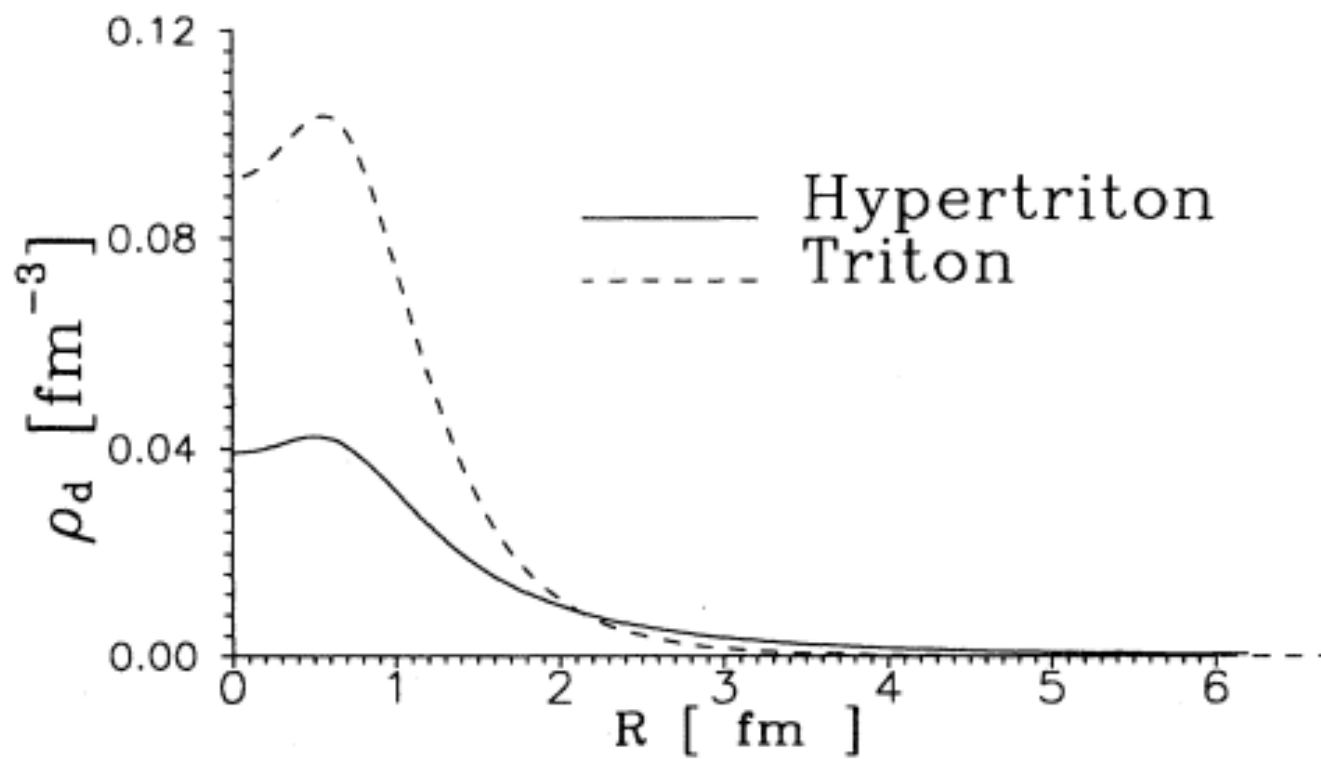
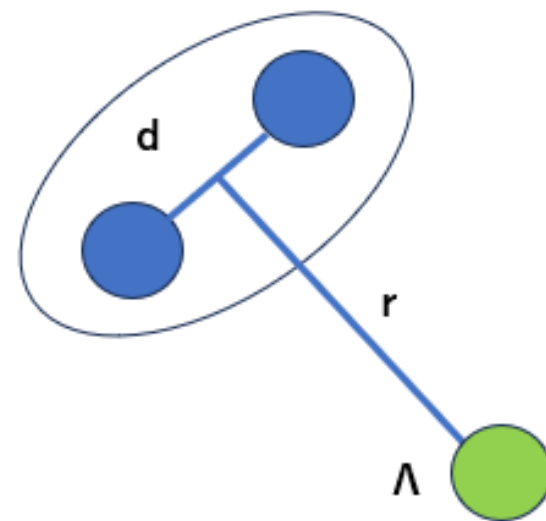
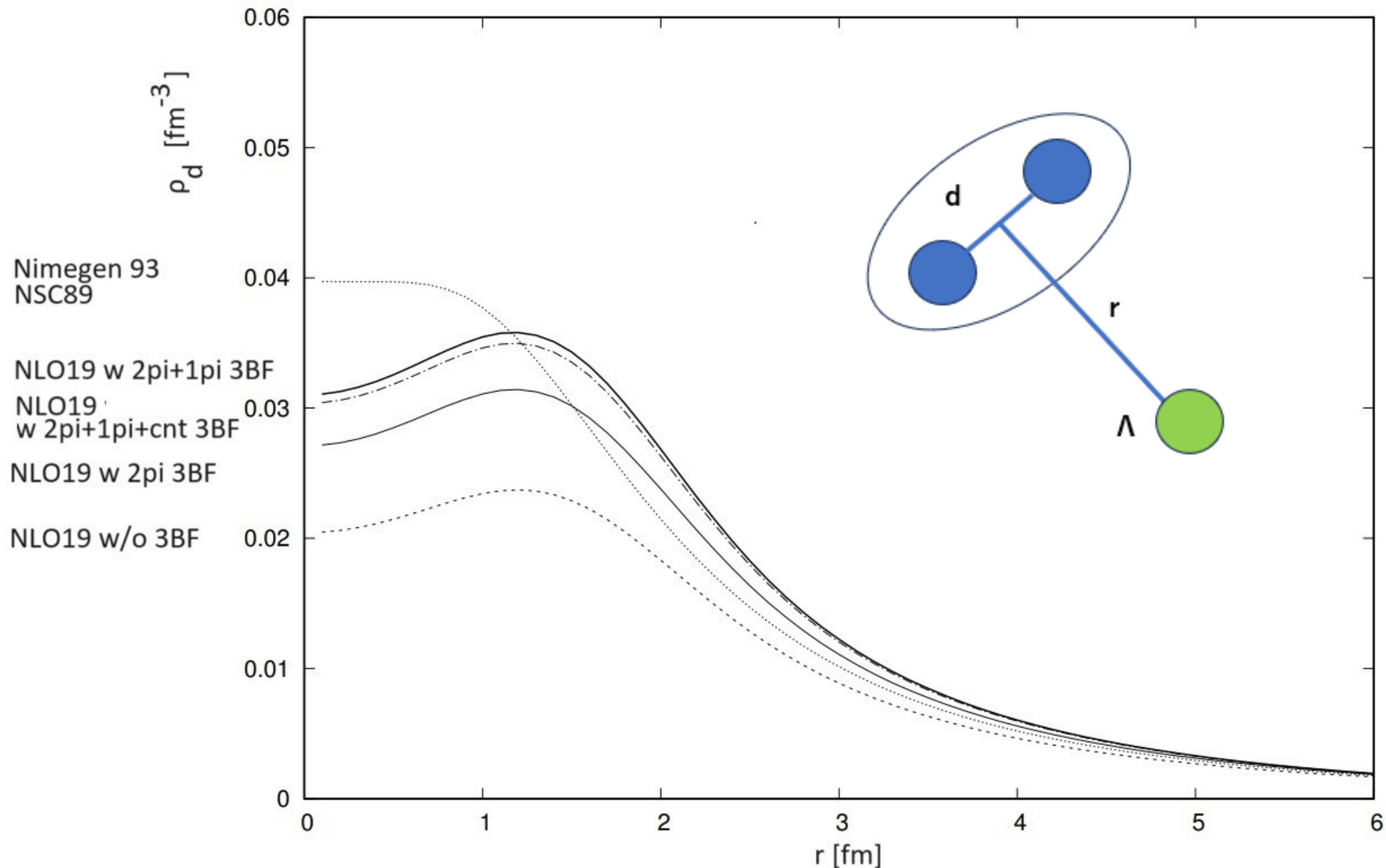


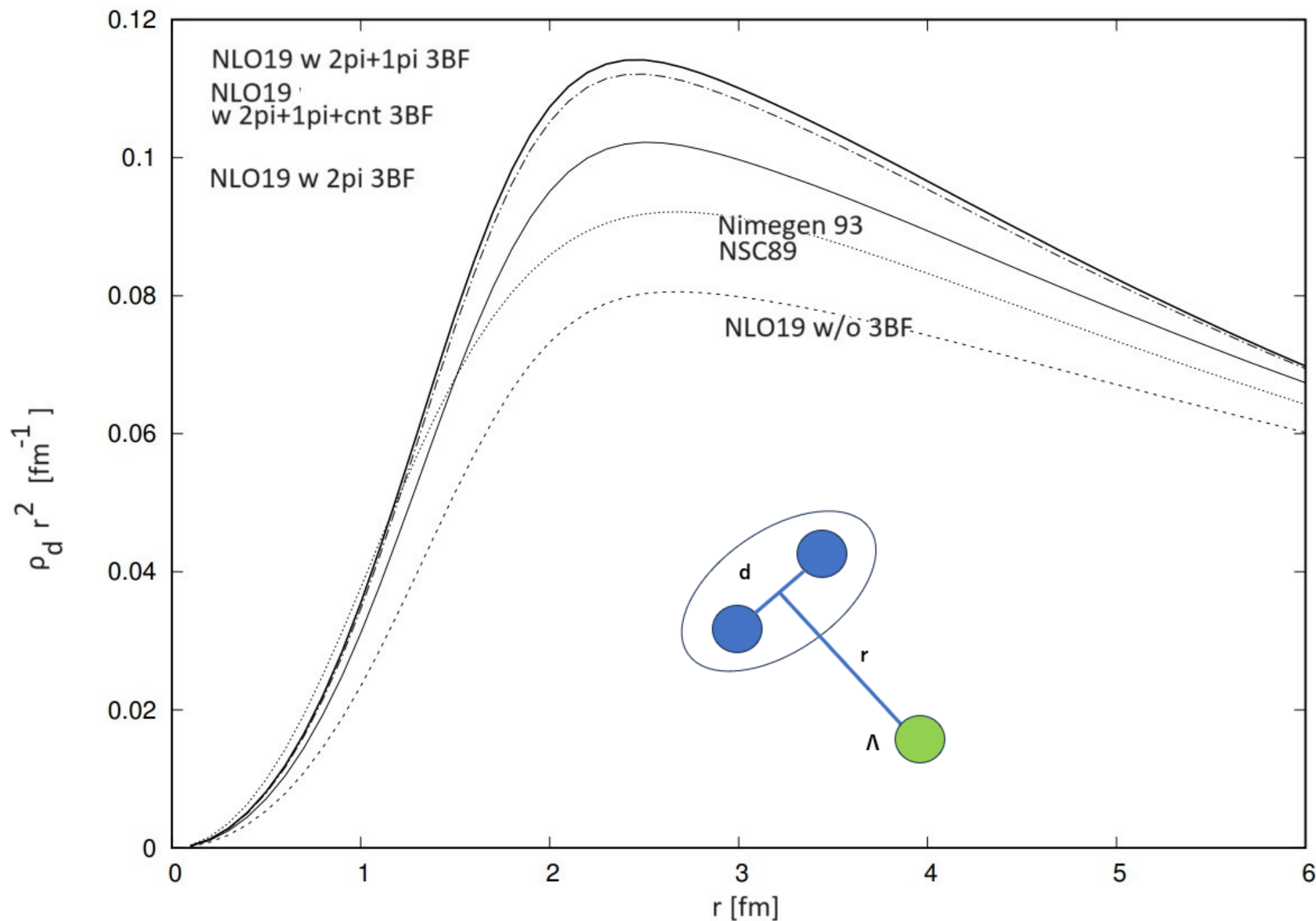
FIG. 11. Comparison of the deuteron overlap functions $\rho_d(r)$ for the triton and the hypertriton.

we find $P_d = 0.448$ for the triton and $P_d = 0.987$ for the hypertriton



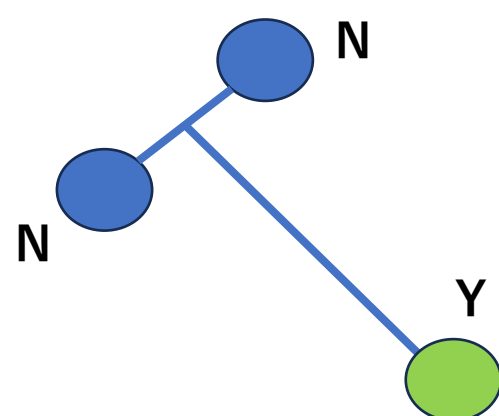
$$P_d \equiv \int_0^\infty dr r^2 \rho_d(r) , \quad (13)$$



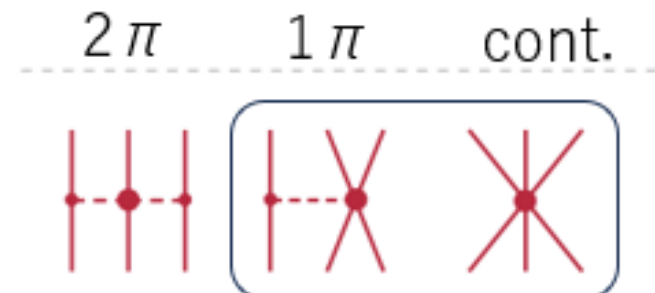


Expectation values of the Kinetic energies in Hypertriton (Unit in MeV)

	Nijm93 NSC89	N^4LO+ $NLO19$	N^4LO+ $NLO19$ 2π 3BF	N^4LO+ $NLO19$ $2\pi+1\pi$ 3BF	N^4LO+ $NLO19$ $2\pi+1\pi+cnt.$ 3BF
N-N relative	20.27 (0.23)	16.46 (0.12)	16.85 (0.17)	17.13 (0.20)	17.07 (0.19)
(NN)-Y relative	2.20 (0.80)	1.87 (0.40)	2.50 (0.72)	2.87 (0.65)	2.80 (0.63)
Total	23.51	18.85	20.07	20.83	20.70



Inside of () is the contribution from Σ particle.



Conclusion and Outlook

- **For the first time**, we performed Faddeev calculations of Hypertriton including three-body forces.
- The YNN 3 body force had a **non-negligible** effect on the binding energy.
- Since the YN potential of **SMS** is NNLO, it is now possible to include 2π -type three-body forces **consistently**.
- (It is now possible to include three-body forces in the NCSM of medium-mass hypernuclei.)

This work is supported by Japan Society for the Promotion of Science (JSPS) KAKENHI Grants No. JP19K03849 and No. JP22K03597.

Thank You for your attention.

Next pages are for discussion after presentation.

Table 4 Scattering lengths (a) and effective ranges (r) for singlet (s) and triplet (t) S -waves (in fm), for ΛN , ΣN with isospin $I = 1/2, 3/2$, and for $\Sigma^+ p$ with inclusion of the Coulomb interaction

Λ [MeV]	SMS NLO			SMS N ² LO			NLO13		NLO19	
	500	550	600	500	550	600	600	600	600	600
$a_s^{\Lambda N}$	-2.80	-2.79	-2.79	-2.80	-2.79	-2.80	-2.91	-2.91	-2.91	-2.91
$r_s^{\Lambda N}$	2.87	2.72	2.63	2.82	2.89	2.68	2.78	2.78	2.78	2.78
$a_t^{\Lambda N}$	-1.59	-1.57	-1.56	-1.56	-1.58	-1.56	-1.54	-1.54	-1.41	-1.41
$r_t^{\Lambda N}$	3.10	2.99	3.00	3.16	3.09	3.17	2.72	2.72	2.53	2.53
$\text{Re } a_s^{\Sigma N (I=1/2)}$	1.14	1.15	1.10	1.03	1.12	1.06	0.90	0.90	0.90	0.90
$\text{Im } a_s^{\Sigma N}$	0.00	0.00	0.00	0.00	0.00	0.00	0.00	0.00	0.00	0.00
$\text{Re } a_t^{\Sigma N (I=1/2)}$	2.58	2.42	2.31	2.60	2.38	2.53	2.27	2.27	2.29	2.29
$\text{Im } a_t^{\Sigma N}$	-2.60	-2.95	-3.09	-2.56	-3.26	-2.64	-3.29	-3.29	-3.39	-3.39
$a_s^{\Sigma N (I=3/2)}$	-4.21	-4.05	-4.11	-4.37	-4.19	-4.03	-4.45	-4.45	-4.55	-4.55
$r_s^{\Sigma N}$	3.93	3.89	3.75	3.73	3.89	3.74	3.68	3.68	3.65	3.65
$a_t^{\Sigma N (I=3/2)}$	0.46	0.47	0.47	0.38	0.44	0.41	0.44	0.44	0.43	0.43
$r_t^{\Sigma N}$	-5.08	-4.74	-4.82	-5.70	-4.96	-5.72	-4.59	-4.59	-5.27	-5.27
$a_s^{\Sigma^+ p}$	-3.41	-3.30	-3.44	-3.47	-3.39	-3.25	-3.56	-3.56	-3.62	-3.62
$r_s^{\Sigma^+ p}$	3.75	3.73	3.59	3.61	3.73	3.65	3.54	3.54	3.50	3.50
$a_t^{\Sigma^+ p}$	0.51	0.52	0.52	0.41	0.48	0.45	0.49	0.49	0.47	0.47
$r_t^{\Sigma^+ p}$	-5.46	-5.12	-5.19	-6.74	-5.50	-6.41	-5.08	-5.08	-5.77	-5.77

Semilocal Momentum-Space regularized (*from Evgeny's note*)

2014: The SFR removes the unphysical short-range components but one also distorts some good long-range physics... Can one do better?

⇒ local regularization in r-space EE, Krebs, Meißner, EPJA 51 (15) 53
PRL 115 (15) 122301



2018: The r-space regulator turned out to be inconvenient for 3N forces and currents

⇒ local regularization in momentum space Reinert, Krebs, EE, EPJA (18) 85

$$V_{1\pi}(q) = \frac{\alpha}{\vec{q}^2 + M_\pi^2} e^{-\frac{\vec{q}^2 + M_\pi^2}{\Lambda^2}} + \text{subtraction},$$

$$V_{2\pi}(q) = \frac{2}{\pi} \int_{2M_\pi}^{\infty} d\mu \mu \frac{\rho(\mu)}{\vec{q}^2 + \mu^2} e^{-\frac{\vec{q}^2 + \mu^2}{2\Lambda^2}} + \text{subtractions}$$

Semilocal **M**omentum-**S**pace regularized (from Evgeny's note)

